Temperature Dependence of Solvation Dynamics of Probe Molecules in Methanol-Doped Ice and in Liquid Ethanol

Anna Uritski and Dan Huppert*

Raymond and Beverly Sackler Faculty of Exact Sciences, School of Chemistry, Tel Aviv University, Tel Aviv 69978, Israel

Received: June 19, 2007; In Final Form: August 2, 2007

We have studied the solvation statics and dynamics of coumarin 343 and a strong photoacid (pK^* ∼ 0.7) 2-naphthol-6, 8-disulfonate (2N68DS) in methanol-doped ice (1% molar concentration of methanol) and in cold liquid ethanol in the temperature range of 160−270 K. Both probe molecules show a relatively fast solvation dynamics in ice, ranging from a few tens of picoseconds at about 240 K to nanoseconds at about 160 K. At about 160 K in doped ice, we observe a sharp decrease of the dynamic Stokes shift of both coumarin 343 and 2N68DS. Its value is approximately only 200 cm^{-1} at ∼160 K compared to about 1100 cm^{-1} at $T \geq 200$ K (at times longer than $t > 10$ ps). We find a good correlation between the inefficient and slow excited-state proton-transfer rate at low-temperature ice, $T < 180$ K, and the dramatic decrease of the solvation energy, as measured by the dynamic band shift, at these low temperatures. We find that the average solvation rate in ice is similar to its value in liquid ethanol at all given temperatures in the range of 200−250 K. The surprisingly fast solvation rate in ice is explained by the relatively large freedom of the water hydrogen rotation in ice I_h.

Introduction

Solvation statics and dynamics have been studied extensively.[1−7] Ultrashort laser pulses of femto- and picosecond time duration have been used during the last two decades to study the solvation process on a femto- and picosecond time scale. In these studies, the solvation dynamics were monitored via the time-dependent spectral shift of the fluorescence band of a probe molecule dissolved in the solvent. Most of the studies of solvent dynamics had been conducted in neat polar liquid solvents. Richert[8] studied the solvation dynamics of a probe molecule in viscous liquids and glass materials near their glass transition. It was found[8] that macroscopic static and dynamic dielectric properties fit the solvation dynamics spectroscopic measurements.

In this paper, we have extended the traditional solvation study. First, we conducted the study of solvation in the solid state. The solid examined in our study was ice. Second, we used two probe molecules, coumarin 343 (c343) (a known coumarin dye probe molecule) and a photoacid molecule, 2-naphthol-6,8-disulfonate (2N68DS). The motivation for studying this particular system, 2N68DS in ice, stems from our recent studies of excited-state proton transfer in ice. In particular, we found that the change in the rate of proton transfer ($-\mathrm{d} \ln k_{PT}/\mathrm{d}T$) at low temperatures, $T < 180$ K, strongly increases.

The physics of ice[9−12] has been studied extensively for many years. Electrical conductivity measurements that had been conducted in the 1960s by Eigen and co-workers[13] provided a large mobility for proton transfer in ice, 10−100 times larger than that in water. Further measurements showed that the proton low-frequency mobility in ice at approximately 263 K is about a factor of 2 smaller than that in super-cooled water[11,14] at the same temperature.

Pauling[15] proposed the structure of the ice I_h where the oxygen atoms are arranged on a hexagonal lattice. Each oxygen atom has four nearest neighbors at the corners of a regular tetrahedron. The hydrogen atoms are covalently bonded to the nearest oxygen to form H_2O molecules, and their molecules are linked to one another by hydrogen bonds, each molecule offering its hydrogens to two other molecules and accepting hydrogens bonds from another two. The essential feature of Pauling's model is that there does not exist a long-range order in the orientation of the H_2O molecules or of the hydrogen bonds.

The theory of Jaccard[16] (proposed in 1959) is still being used to explain the electrical conduction in ice. According to Jaccard's theory, the electrical properties of ice are large due to two types of defects within the crystal structure. Ion defects are produced when a proton moves from one end of the bond to the other, thus creating a H_3O^+, OH^- ion pair. Conduction is then possible by means of successive proton jumps. Bjerrum defects[17] are orientational defects caused by the rotation of a water molecule to produce either a doubly occupied bond (D defect) or a bond with no protons (L defect).

Solvation dynamics would not have been observed if the water molecule motion had been totally frozen in the ice structure. This also stands for electrical conductance and the excited-state proton-transfer reaction. Therefore, solvation dynamics is associated with electrical mobility, crystal imperfection, and the creation and annihilation of the four defects. Podeszwa and Buch[18] studied the structure and dynamics of orientational defects in ice by molecular dynamics simulation. They found that the defect structure is quite different from the one originally proposed by Bjerrum.[17] Two basic structures were identified for the D defect, whereas one dominant structure was obtained for the L defect. Typically, one water molecule in an L defect is displaced ∼1 Å from the crystal lattice site. Defect jumps occur via vibrational phase coincidence.

In a recent study in the ice phase, we observed that below 180 K, excited-state proton transfer is inefficient and, therefore,

* To whom correspondence should be addressed. E-mail: huppert@tulip.tau.ac.il. Phone: 972-3-6407012. Fax: 972-3-6409293.

10.1021/jp0747454 CCC: $37.00
Published on Web 09/22/2007

the RO^- emission band (the deprotonated form of the photoacid) tends to disappear around this temperature. As we will show in this study, the solvation dynamic of both coumarin 343 and 2N68DS at 180 K and below is slow and comparable to the excited-state lifetime. Even more so, the total dynamical solvation energy red shift during the excited-state lifetime is rather small, about 200 cm^{-1} at 160 K, while its value at $T >$ 200 K is about 1100 cm^{-1}. The main results of the current study are in good agreement with our previous study.[19] There, we proposed that at sufficiently low temperature, the proton transfer cannot take place because a prerequisite condition to the actual proton translocation process is some hydrogen-bonding rearrangements, which should take place prior to the actual proton transfer. The solvation dynamics experiments in this study indicate that, indeed, some hydrogen-bond rearrangements are inhibited at sufficiently low temperatures and, thus, the proton-transfer process cannot take place.

Experimental Section

Time-resolved fluorescence was measured by time-correlated single-photon counting (TCSPC) technique. The method has large sensitivity and a large dynamic range. It is especially useful when low-intensity illumination is an important criterion in fluorescence decay measurements.

For excitation, we used a cavity-dumped Ti:sapphire femtosecond laser, Mira, Coherent, which provides short, 80 fs pulses of variable repetition rate, operating at the SHG and the THG frequencies over the spectral range of 380−400 nm and 250−290 nm, with the relatively low repetition rate of 500 kHz. The TCSPC detection system is based on a Hamamatsu 3809U photomultiplier and an Edinburgh Instruments TCC 900 computer module for TCSPC. The overall instrumental response was about 35 ps (fwhm). Measurements were taken at a 10 nm spectral width. The observed transient fluorescence signal, $I(t)$, is a convolution of the instrument response function (IRF), $I_0(t)$, with the theoretical decay function. The excitation pulse energy was reduced by neutral density filters to about 10 pJ. We checked the absorption of the sample prior to and after time-resolved measurements. We could not find noticeable changes in the absorption spectra resulting from sample irradiation.

Steady-state fluorescence spectra were taken using a FluoroMax (Jobin Yvon) spectrofluorimeter and a miniature CCD spectrograph CVI MS-240 or EPR 2200 (Stellarnet). The coumarin 343 was purchased from Excitation, and 2-naphthol-6,8-disulfonate (2N68DS) was purchased from Kodak. Perchloric acid, 70% reagent grade, was purchased from Aldrich. For steady-state fluorescence measurements, we used photoacid solutions of $\sim 2 \times 10^{-5}$ M. For transient measurements, the sample concentrations were between 2×10^{-4} and 2×10^{-5} M. Deionized water had a resistance of >10 MΩ. Fluka's analytical grade methanol was used, and all chemicals were used without further purification. The solution pH was about 6.

The temperature of the irradiated sample was controlled by placing the sample in a liquid N_2 cryostat with a thermal stability of approximately ±1.5 K.

In the solid phase, the photoacids tend to aggregate, and as a consequence, the luminescence intensity in frozen samples is strongly reduced. The net result is an unreliable time-resolved emission measurement in the ice-phase, of both acid (ROH*) and base (RO^-*) forms. The aggregation problem of the photoacids in the ice phase was unnoticed when a small amount of methanol, ~1% mole fraction, had been added to the solution.

Ice samples were prepared by first placing the cryogenic sample cell at a temperature of about 273 K for about 20 min. The second step involved a relatively rapid cooling (10 min) to a low temperature. The sample subsequently froze within 5 min. To ensure ice equilibration prior to the time-resolved measurements, the sample temperature was kept constant for another 30 min.

Results

Solvatochromism of Photoacids. Many compounds exhibit solvatochromic spectral changes, both in their absorption spectrum and in their fluorescence, and/or phosphorescence spectra. The Kamlet−Taft[20,21] solvatochromic scale uses several parameters to describe and quantify the various contributions. The π^* scale is an index of solvent dipolarity/polarizability, which measures the ability of the solvent to stabilize a charge or dipole by virtue of its dielectric effect. The a scale of solvent hydrogen-bond-donor (HBD) acidities describes the ability of the solvent to donate a proton in a solvent-to-solute hydrogen bond. The β scale of hydrogen-bond-acceptor (HBA) basicities provides a measure for the ability of solvents to accept a proton (i.e., donate an electron pair in a solute-to-solvent hydrogen bond).

Generally, the spectral position of a band in solution is given by

$$\nu_0 = \nu_0 + p\pi^* + a\alpha + b\beta \quad (1)$$

The coefficients p, b, and a are interpreted as solute properties; p is related to the solute dipole moment; b measures its propensity to donate a HB to the solvent; and a describes its tendency to accept a HB from the solvent.

In the past, we studied the solvatochromism of two photoacids.[22,23] Excitation and emission fluorescence spectra of 2-naphthol and 2-methoxynaphthalene were measured in a series of pure solvents.[23] The spectral shifts were correlated by the Kamlet−Taft parameters (π^*, β, and α). From the π^* dependence, we calculated that both molecules have a small dipole moment in their ground electronic state, which increases in the excited (S_1) state. The majority of the Stokes shift is attributed to hydrogen bonding rather than to dipole−dipole interactions. By comparing the shifts for the two compounds, it was found that the β dependence in 2-naphthol is attributed to a hydrogen bond donated by its hydroxylic hydrogen atom to the solvent. This bond becomes stronger upon excitation and, hence, produces a bathochromic shift. Dependence was found on α only in the excitation spectrum, indicating that protic solvents stabilize the ground state by donating a hydrogen bond to the hydroxylic oxygen. This bond breaks following excitation to S_1 but re-forms following proton transfer. The value of the Kamlet−Taft p and b coefficients for the emission spectrum of 2-naphthol are $p = -450$ cm^{-1} and $b = -800$ cm^{-1}.[23]

5-Cyano-2-naphthol (5CN2OH) is a strong photoacid, pK^* ~ -1.[22] The value of the Kamlet−Taft coefficients for this strong photoacid were found to be much larger than those for 2-naphthol,[23] $p = -1600$ cm^{-1} and $b = -1820$ cm^{-1}. Figure 1 shows the steady-state emission of 2N68DS in several polar and hydroxylic solvents. 2N68DS is a salt, and therefore, it strongly limits the number of solvents that we could use in the determination of the Kamlet−Taft correlation. We determined the Kamlet−Taft coefficients for 2N68DS in this study using the ROH band peak position. We deduced the Kamplet−Taft coefficients using a multilinear regression procedure for the ROH emission band peak position of the 2N68DS.[23] The values of the coefficients are $p = -1200$ cm^{-1}, $b = -1100$ cm^{-1}, and $a = -1300$ cm^{-1}. The Kamlet−Taft p and b coefficients of

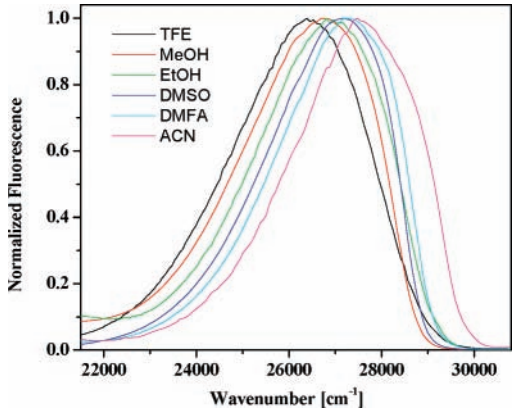

Figure 1. Steady-state emission of 2N68DS in several polar and hydroxylic solvents.

2N68DS (pK^* ≃ 0.7) are in between the small values of the weaker photoacid 2-naphthol (pK^* ≃ 2.7) and the large values of the super photoacid 5CN2OH (pK^* ≃ −1).

For 2N68DS, we found that the Stokes shift also depends on α, indicating that a hydrogen bond from the solvent to the photoacid is important for the excited-state stabilization of the ROH form of 2N68DS. For both 2-naphthol and 5CN2OH, it was found that α = 0. The relatively large value of α in the case of 2N68DS may arise from the hydrogen-bond formation between the solvent hydrogens with the ionic solfonate oxygens.

The Solvatochromism of C343 was studied in homogeneous media and in aqueous and nonaqueous reverse micelles (RMs) by Correa and Levinger.[24] They found that the carboxylic acid group causes C343 to display greater sensitivity to the β than to the π^* polarity parameter; this sensitivity increases in the excited state, while the dependence on α vanishes. This demonstrates that C343 forms a stable H-bond complex with solvents with high H-bond-acceptor ability (high β) and low H-bond-donor character (low α). The values of the Kamlet−Taft parameters for C343 emission are $p = -1100$ cm^{-1} and $b = -1610$ cm^{-1}. As in the case of 2-naphthol, they found $a \approx 0$ for the emission and about +200 cm^{-1} for the absorption spectrum.

To summarize this subsection, while most of the solvation dynamics and energetics efforts are to explain the results in terms of dipolar interaction, for the specific fluorescent probes of this study, the main contribution to excited-state solvation energy is gained by the hydrogen bonding of the fluorophore hydroxyl group with the solvent oxygen. This might be the first step in the more complex reaction of the excited-state proton transfer.

Steady-State Emission. The fluorescence spectrum of 2N68DS in liquid water and in ice at high temperatures, $T > 180$ K, consists of two structureless broad bands (∼ 40 nm fwhm). The emission band maximum of the acidic form (ROH*) in water is at about 370 nm, and the alkaline form (RO$^-$*) is at 470 nm for 2N68DS. At 370 nm, the overlap of the two luminescence bands is rather small. The RO$^-$ emission band intensity is much stronger than the ROH band in water and in ice at high temperatures, $T > 250$ K. This large difference in the band intensity is due to a fast proton-transfer rate (40 ps at $T = 290$ K) from the excited photoacid to a nearby water molecule.

Figure 2 shows the steady-state emission spectra of coumarin 343 at various temperatures in ethanol and in methanol-doped ice (1% mole). The peak position of the emission spectrum exhibits a strong temperature dependence in both media. On the energy scale, the emission band position increases as the temperature decreases. In general, an emission blue band shift

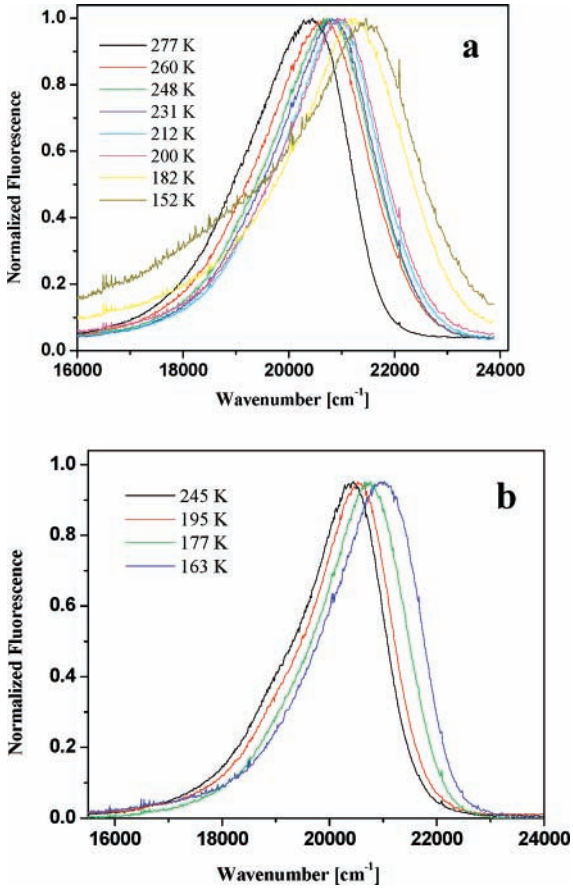

Figure 2. Steady-state emission spectra of coumarin 343 at various temperatures; (a) in methanol-doped ice (1% mole) and (b) in ethanol.

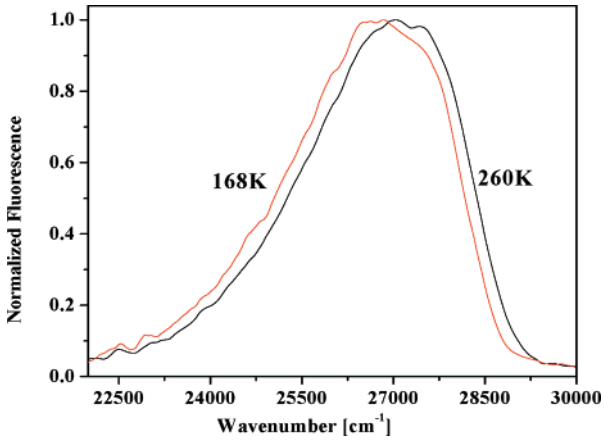

Figure 3. The steady-state emission spectra of 2N68DS at various temperatures in ethanol.

is expected in the case of the dielectric constant decrease. However, this is not the case for hydroxylic solvents like alcohol and ice. In these solvents, the dielectric constant increases with the temperature decrease, and thus, we expect an emission red shift while the temperature decreases. If the solute−solvent interaction is quadratic, then, depending on the interaction parameters, the emission band shift can change direction, and a blue shift can be expected.[25]

Figure 3 shows the steady-state emission spectra of the ROH band of 2N68DS at various temperatures in methanol-doped ice. The peak of the emission band shifts only slightly to the blue as the temperatures decrease.

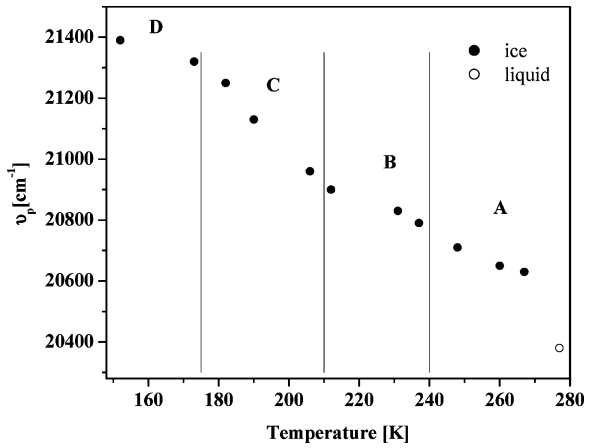

Figure 4. The peak position of the emission band of coumarin 343 in methanol-doped ice as a function of temperature.

Figure 4 shows the emission band peak position as a function of temperature for coumarin 343 in methanol-doped ice. In the liquid state, at room temperature, the band peak position is at about 20400 cm^{-1} (490 nm). The band peak position shows an abrupt blue shift of ~200 cm^{-1} upon sample freezing. The change in the band position as a function of the temperature has approximately a concave shape. As the temperature is lowered, the absolute value of $\Delta\nu/\Delta T$ becomes larger. At a temperature below about 170 K, the band position is almost insensitive to the temperature. In addition, at about 180 K, a new broad band appears in the spectrum at about 550 nm. As the temperature is lowered, the new red band intensity gets larger.

Time-Resolved Emission. The solvent polarization relaxation is related to the relaxation function defined by a normalized spectral shift correlation function $S(t)$

$$S(t) = \frac{\nu(t) - \nu(\infty)}{\nu(0) - \nu(\infty)} \tag{2}$$

where $\nu(0)$, $\nu(t)$, and $\nu(\infty)$ represent the frequency of the intensity maximum of the fluorescence spectrum immediately after a photon excitation, at some time t after excitation, and at a time sufficiently long to ensure that the excited-state solvent configuration is at equilibrium. Thus expressed, the frequencies need not be referenced to their (usually unknown) gas-phase values. For a single Debye dielectric relaxation, $S(t)$ decays exponentially with a time constant of τ_S. In general, it was found that the solvation process is bimodal. In a large number of solvation dynamics experimental and simulation studies, it was found that about 50% of the solvation energy is gained on a short time scale $\leq$100 fs. The rest of the solvation energy is gained on about a 1 ps time scale for nonassociative liquids, whereas for associative liquids, like alcohols, the average decay time of this long solvation component increases (a few picoseconds to about a few hundred picoseconds), depending on the aliphatic chain length.[26,27] The time constant of the long time component of the solvation τ_S is comparable to τ_L, the longitudinal dielectric relaxation time

$$\tau_L = (\epsilon_\infty/\epsilon_0)\tau_D \tag{3}$$

Where ϵ_∞ and ϵ_0 are the dielectric constants at high and low frequencies, and τ_D is the dielectric relaxation time measured by the dielectric response of the media. In highly polar solvents, $\tau_L \ll \tau_D$, and the decrease in the solvation time scale from the solvent Debye time is a manifestation of the cooperative nature

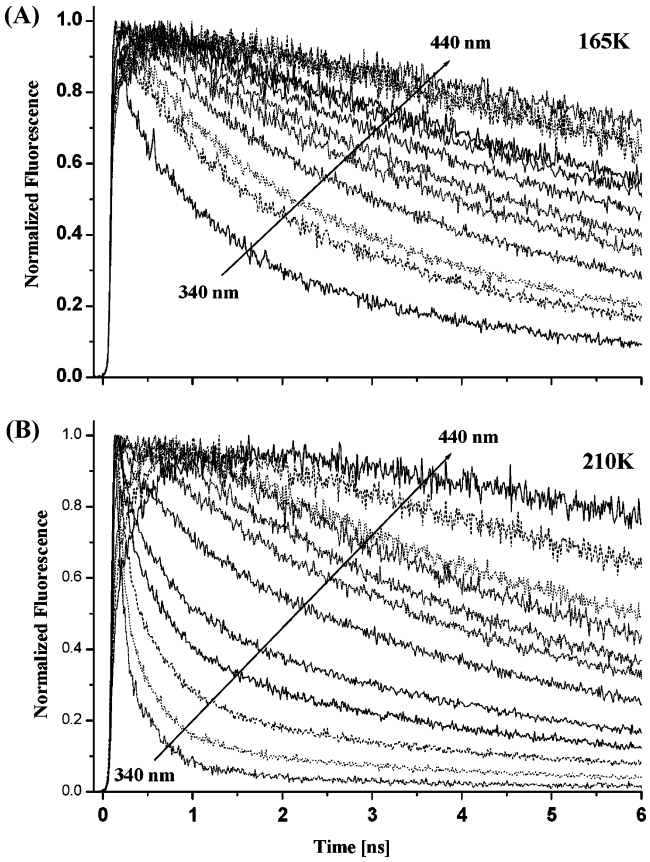

Figure 5. Time-resolved emission signal of 2N68DS in methanol-doped ice measured at 10 nm intervals in the spectral range of 340−440 nm at two temperatures; (A) at 165 K and (B) at 210 K.

of the solvation response. The average solvation time defined by eq 4 is used for comparison of complex decay profiles

$$\langle\tau\rangle \equiv \int_0^\infty S(t)\mathrm{d}t \tag{4}$$

$S(t)$ analytically represented as a sum of exponentials or as a "stretched" exponential function is

$$S(t) = \mathrm{e}^{-(t/\tau)^\alpha} \tag{5}$$

Further, since the magnitude of the shift is normalized out, different solutes and solvents can be readily compared.

Figure 5 shows the time-resolved emission signal of 2N68DS in methanol-doped ice, measured at 10 nm intervals in the spectral range of 340−440 nm at two temperatures, panel A 165 K and panel B at 210 K.

The experimental time-resolved spectra were constructed by a procedure given by Maroncelli and co-workers.[1] Only the long time components (>20 ps) were accurately time-resolved in this study. The time-resolved emission data collected at 10 nm intervals were fitted to a sum of exponentials using a convoluted procedure with the system IRF.

Figure 6 (panels A and B) shows the normalized solvation correlation function $S(t)$ for 2N68DS in methanol-doped ice at three temperatures. The decay of the $S(t)$ of 2N68DS is nonexponential. We fit the data with a three-exponential function. The time constant of the short components is around 100 ps. The time constant of the long time components strongly depends on the temperature. The relative amplitude of the short

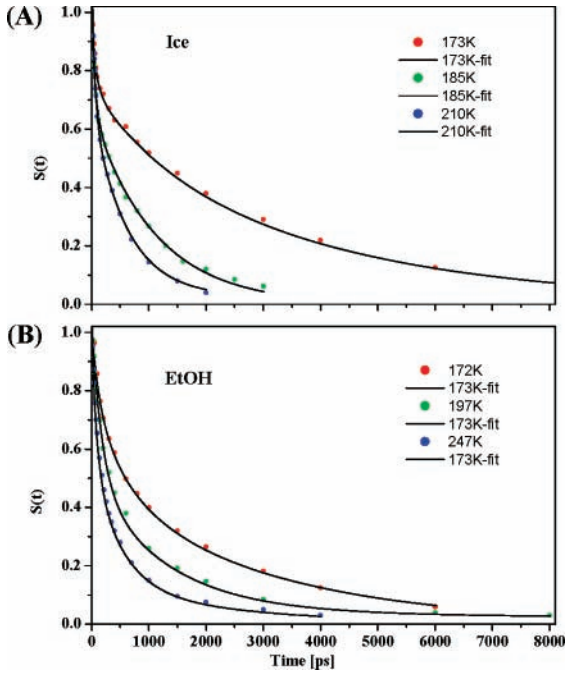

Figure 6. The normalized solvation correlation function $S(t)$ of 2N68DS in (A) methanol-doped ice and (B) ethanol at three temperatures.

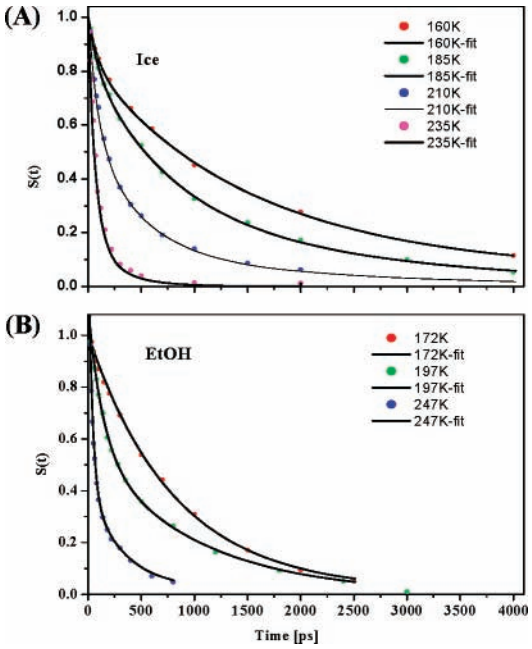

Figure 7. $S(t)$ of coumarin 343 in (A) methanol-doped ice and (B) ethanol.

time components decreases as the temperature decreases. The average solvation time $<\tau_{average}>$ increases as the temperature decreases.

Figure 7 shows similar results for the $S(t)$ of coumarin 343 in methanol-doped ice and in ethanol. As in the case of 2N68DS, the solvation dynamics of C343 in ice depends on the temperature. The long time components increase from a few hundreds of picoseconds at 235 K to a few nanoseconds at 185 K. The activation energies of the average solvation time of C343 and 2N68DS in ice are similar, $E_a^s \approx 18$ kJ/mol.

Table 1 summarizes the fitting parameters of $S(t)$ of 2N68DS in methanol-doped ice and in ethanol, and Table 2 shows the fitting parameters of $S(t)$ of coumarin 343 in methanol-doped ice and ethanol.

TABLE 1: Fitting Parameters of $S(t)$ of 2N68DS

a. Methanol-Doped Ice

T [K]	a_1	τ_1 [ps]	a_2	τ_2 [ps]	a_3	τ_3 [ps]	$\tau_{average}$ [ps]
210	0.43	50	0.57	600			352
185	0.31	70	0.69	1100			777
173	0.26	70	0.2	1200	0.54	4000	2400
160	0.340	170	0.1	900	0.56	2300	1465

b. Ethanol

T [K]	a_1	τ_1 [ps]	a_2	τ_2 [ps]	a_3	τ_3 [ps]	$\tau_{average}$ [ps]
192	0.435	90	0.435	500	0.13	2000	470
172	0.54	180	0.46	1300			695
165	0.245	150	0.283	600	0.471	3000	1620

TABLE 2: Fitting Parameters of $S(t)$ of C343

a. Methanol-Doped Ice

T [K]	a_1	τ_1 [ps]	a_2	τ_2 [ps]	a_3	τ_3 [ps]	$\tau_{average}$ [ps]
235	0.606	55	0.303	120	0.09	300	96
210	0.409	90	0.55	450	0.13	2000	550
185	0.166	90	0.555	750	0.277	2500	1125
160	0.15	90	0.5	1250	0.25	3500	1680

b. Ethanol

T [K]	a_1	τ_1 [ps]	a_2	τ_2 [ps]	a_3	τ_3 [ps]	$\tau_{average}$ [ps]
247	0.7	37	0.263	300	0.035	1500	126
197	0.5	140	0.5	1000	0.02	1500	580
172	0.97	800	0.03	5000			885

At the temperature interval of 240−180 K, in methanol-doped ice, we observe a time-dependent red shift of the ROH emission band of 2N68DS of about 1100 cm^{-1} in the time interval of 10 ps−10 ns. A similar band shift is observed in the same solid for coumarin 343. At about 240 K, the decay of the normalized solvent correlation function $S(t)$ can be described approximately by two exponential functions, where each component has about the same amplitude. At about 240 K, the average decay time of $S(t)$ is about $<\tau> \simeq 80$ ps, while at $T = 180$ K, $<\tau> \simeq 2$ ns. For coumarin 343, we find a similar average time and a somewhat smaller total band shift of about 1000 cm^{-1} for the decay of $S(t)$. Below 180 K, the solvation energy (determined by the total band shift $(\upsilon_0 - \upsilon_\infty)$) strongly decreases as the temperature decreases. At about 150 K, the solvation energy drops to about 200 cm^{-1}, compared to 1100 cm^{-1} at temperatures higher than 200 K. Figure 8 shows the peak position υ_p of the time-resolved emission spectrum of C343 for several temperatures in ice as a function of time. As seen in this figure, at high temperature, the total observed shift is of ~1000 cm^{-1}. At lower temperatures, $T < 200$ K, the total shift $\upsilon_0 - \upsilon_\infty$ decreases as the temperature decreases. This finding fits the observation of our previous study[19] that at sufficiently low temperatures ($T < 180$ K), the rate of the excited-state proton transfer shows a rather strong dependence on temperature. As a consequence of the slow proton-transfer rate, the yield of the proton-transfer process is low, and the RO^- emission band is missing in the spectrum.

Discussion

The main points found in this study are as follows:

1. Solvation dynamics and statics are easily observed in methanol-doped ice for both coumarin 343 and 2N68DS.

2. At sufficiently low temperature, the solvation dynamics in methanol-doped ice is rather slow and comparable with the excited-state lifetime.

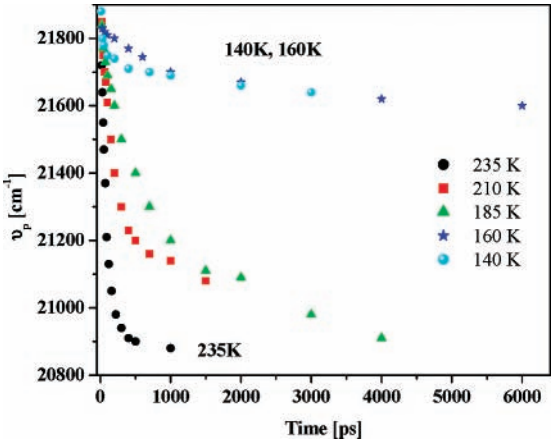

Figure 8. The band position υ_p of C343 at several temperatures in ice as a function of time. The large decrease in the solvation energy at low temperature should be noted.

3. At sufficiently low temperature (below 180 K), the total solvation energy drops drastically as the temperature further decreases.

4. At low temperatures, $T < 190$ K, in coumarin 343 methanol-doped ice samples, a new broad emission band appears at about 550 nm.

5. Below 160 K in methanol-doped ice, the time-resolved emission of 2N68DS shows a significant nonradiative nonexponential decay. This process also decreases the absolute intensity of the steady-state emission of the ROH band and, hence, complicates the data analysis below 160 K.

From this current solvation study, we found that the solvation dynamics indeed slows down as the temperature decreases. At sufficiently low temperatures, the solvation time reaches the value of the excited-state lifetime. Moreover, we found that the total solvation energy for both C343 and 2N68DS drops dramatically at a turnover temperature of about 160 K. In a previous study,[19] we measured the steady-state emission of HPTS at various temperatures in the range of 90−300 K. We fitted the ROH emission band of HPTS with four vibronic bands with a spacing of about 1200 cm^{-1}. At the lowest temperature range, the bandwidth was 1150 cm^{-1}, and each band was well separated from its neighbor. The bandwidth and position started to change only above 125 K. The red shift and the bandwidth increased monotonically with temperature increase. At temperatures above 170 K, within a small interval of about 20 K, the bandwidth and the peak position of the ROH spectrum of HPTS exhibited a large change of about 300 cm^{-1} compared to a total red shift and a bandwidth increase of about 700 cm^{-1}. The large change in the ROH spectrum at about 180 K was accompanied by the appearance of the RO$^-$ band ($T > 180$ K). These finding were consistent with the time-resolved solvation dynamics in the methanol-doped ice of this study. At about the same temperature below 180 K, the dynamic part of the solvation energy dropped from about 1000 (190 K) to about 200 cm^{-1} (160 K) for both C343 and 2N68DS.

The Relation of Solvation Dynamics and Energetics with Excited-State Proton Transfer. Understanding solvation and how chemical processes are modified by a solvent environment has been a long-standing goal in chemistry. Recent emphasis on this area has centered on dynamical aspects of the solvent influence, especially with respect to electron- and proton-transfer reactions. The aim is to understand how the finite response time of the polar solvent affects such a reaction. Literature concerning the connection between reaction and solvation dynamics is growing rapidly, and several recent reviews are now available to provide an overview of the field.[24,28] In previous studies, we measured the temperature dependence of the excited-state proton transfer of several photoacids in ice. We found that in ice, both the proton-transfer rate constant k_{PT} and the change in the rate, $-\mathrm{d}(\ln k_{PT})/\mathrm{d}(1/T)$, depend on temperature. Below 180 K, we could not observe the RO$^-$ band in the steady-state emission spectrum of HPTS ($pK^* \simeq 1.3$), and in this study, we found that for 2N68DS ($pK^* \simeq 0.7$) below 160 K, we cannot observe the RO$^-$* band.

In the rest of this subsection, we are attempting to combine the static and dynamic solvation spectroscopic results with the temperature dependence of the excited-state proton-transfer process. In a recent study,[19] we proposed a qualitative model that explains the complex temperature dependence of the proton-transfer rate constant in ice, as we previously proposed for the ESPT process in the liquid state.[29] We assume that the reaction in ice can be described by two coordinates, the generalized solvent coordinate and the proton translocation coordinate. The major contribution to the generalized solvent coordinate in ice is the rotational motion of the hydrogens of the water molecule, creating D and L defects.[11,30] The proton moves to the adjacent hydrogen-bonded solvent molecule only when the solvent configuration brings the system to the crossing point between the two diabatic potential surfaces. When the solvation dynamics is faster than the proton transfer along the proton coordinate, the rate-limiting step is the actual proton transfer. This is the case at high and intermediate temperatures. At a lower temperature, the change in the proton-transfer rate, $-\mathrm{d}(\ln k_{PT})/\mathrm{d}(1/T)$, below 180 K suddenly increases. We explain the sudden turnover feature of the strong decrease in k_{PT} as arising from a limitation on the reaction caused by the restrictions on the H_2O hydrogen reorientations below 180 K.

Therefore, we propose that at a sufficiently low temperature close to the turnover temperature, 160 K (found in this study), the smaller solvation energy strongly affects the excited-state proton-transfer reaction rate, and as a consequence, it strongly decreases. The photoprotolytic process is abruptly arrested, probably because the missing rotational motion of the hydrogen atoms of the H_2O molecule in ice (observed as a decrease in the solvation energy) prevents the proton translocation.

A similar hypothesis is suggested for electron-transfer process. In a recent review article, Matyushov[31] emphasized the importance of the solvent reorganization energy and time scales on the rate of electron transfer in glass-forming solvents close to the glass transition temperature.

It is plausible that the concept of turnover temperature found in the electron-transfer reaction can also be applied to proton transfer in solid methanol-doped ice. The proton-transfer process is inefficient at low temperatures in doped ice because a certain crucial solvent motion is blocked. We attempt to propose another plausible reason for the abrupt change in the solvation dynamics energy below 160 K. In the literature, there is a large number of studies reporting on the properties and structure of a metastable low-temperature phase designated as "ice I_c" in which the oxygens are arranged in a cubic structure of diamond rather than on the hexagonal lattice of the regular I_h.[32] From numerous experiments,[32] it is clear that ice I_c is always metastable, and the temperature at which it transforms to ice I_h is determined by the process of molecular rearrangement. As published in the literature, the temperature of the phase transition between I_c and I_h ranges between 130 and up to 200 K.

The Connection of Solvation Dynamics with the Dielectric Relaxation in Ice. As mentioned above, in liquids, the time constant of the long time component of the solvation τ_S is

comparable to τ_L, the longitudinal dielectric relaxation time (see eq 3). In highly polar solvents, the $\tau_L \ll \tau_D$, and the decrease in the solvation time scale from the solvent Debye time is a manifestation of the cooperative nature of the solvation response.

Richert[8] found a good correlation between the average solvent relaxation times as derived from solvation dynamics experiments and the dielectric relaxation time in several glass-forming materials like 2-MTHF. He was able to follow the solvation dynamics on time scales of about 10 orders of magnitude (picoseconds to seconds) using both the singlet and the triplet states. Richert[8] was able to follow the solvation dynamics in 2-MTHF on time scales of seconds to microseconds using quinoxaline as a probe molecule in its triplet state. Richert et al.[33] were able to cover the fast solvation time in the nanosecond−picosecond scale in the 2-MTHF at the high-temperature range using 4-aminophthalimide in the singlet state.

One can derive a simple equation for the dielectric relaxation time in ice (following Chapter 4 in ref 11). The partial conductivity of each type of the four defects is given by

$$\sigma_i = n_i \mu_i |e_i| \tag{6}$$

where n_i is the number of defects of the i kind, μ_i is their mobility, and e_i is their effective charge.

The combined H_3O^+ and OH^- ionic conductivity is

$$\sigma_\pm = \sigma_1 + \sigma_2 \tag{7}$$

and the Bjerrum conductivity is

$$\sigma_{DL} = \sigma_D + \sigma_L \tag{8}$$

The dielectric relaxation is given by

$$\frac{1}{\tau_D} = \Phi\left(\frac{\sigma_\pm}{e_\pm^2} + \frac{\sigma_{DL}}{e_{DL}^2}\right) \tag{9}$$

where Φ is a geometrical factor related to the O−O distance; $e_\pm$ and e_{DL} are the effective charges of the ionic and Bjerrum defects. Ionic and Bjerrum defects carry effective charges of magnitude $e_\pm$ and e_{DL}, respectively, which must be defined in terms of the effects in their motion. As the net effect of moving a H_3O^+ ion and a D defect along a path is to move a proton of charge e, the effective charges must satisfy the relation

$$e_\pm + e_{DL} = e$$
$$e_\pm = 0.62e \text{ and } e_{DL} = 0.38e \tag{10}$$

In the simplest case of molecular reorientations produced by motion of an L defect (as in pure ice at normal temperatures), the dielectric relaxation is given by

$$\frac{1}{\tau_D} = \frac{\Phi \sigma_4}{e_4^2} \tag{11}$$

where σ_4 and e_4 are the Bjerrum conductivity and the charge of an L defect, respectively.

With some simple derivation, the dielectric relaxation is given by

$$\frac{1}{\tau_D} = \frac{n_4 \nu_4}{3N} \tag{12}$$

N is the number of water molecules per unit volume, whereas ν_4 is the frequency of a single orientational motion of the L defect; $n_4\nu_4$ is the total number of the molecular reorientations occurring in a unit volume per unit time, and thus, apart from a numerical factor, τ_D represents the average between successive reorientations of a single molecule. The solvation dynamics found in this study can be related to ν_4. The problem arises in finding the ratio ν_4/N. The number of defects in our sample close to the photoacid is unknown. In pure ice, the dielectric relaxation time τ_D at about 240 K is very slow, -1.4×10^{-4} s, 7 orders of magnitude longer than the relaxation in water at 294 K and about 8 orders of magnitude longer than τ_S, the long component of the solvation dynamics of water. The small number of defects in pure ice accounts for the 7 order difference between τ_D in water and that in ice.

The dielectric relaxation time of pure ice depends strongly on temperature. The Arrhenius plot of log τ_D versus $1/T$ shows that τ_D increases almost exponentially but exhibits two different slopes. In the high-temperature region, $270 > T > 230$ K, the activation energy corresponds to about 55 kJ/mol,[34] while the slope below 220 K is about half of that, 23 kJ/mol.

In KOH-doped ice prepared from a water solution of about 100 ppm, the dielectric relaxation time at about 200 K decreases by about 3 orders of magnitude compared to that of pure ice.[35] Assuming that doping increases the number of defects in ice, the decrease of the relaxation time is expected according to eq 12. The large increase in the relaxation time with the decreasing ice sample temperature signifies the large decrease in the number of defects as the temperature decreases and the longer relaxation time of a single defect.

The Arrhenius plot of the average solvation time $<\tau>$ of 2N68DS and C343 as a function of $1/T$ in the small temperature range between 235 and 175 K gives an activation energy of about 18 kJ/mol, which is slightly smaller than the activation energy value of τ_D in pure ice in the same temperature range (23 kJ/mol).

Summary and Conclusion

In this study, we focused our attention on the solvation statics and dynamics of a strong photoacid ($pK^* \simeq 0.7$), 2-naphthol-6,8-disulfonate in methanol-doped ice (1% molar concentration of methanol).

In a previous study[19] on intermolecular excited-state proton transfer (ESPT) of several photoacids in methanol-doped ice, we found that at low-temperature, $T < 180$ K, the proton-transfer process rate suddenly decreases strongly as the temperature further decreases. As a consequence, at about 160 K, the deprotonated form (RO^-*) is missing in the steady-state spectrum. We suggested a model for proton transfer that includes two coordinates, a generalized solvent coordinate and the proton translocation coordinate describing the proton transfer to a nearby oxygen of a H_2O molecule. Prior to the proton translocation, the solvent hydrogen bonding and/or D and L defects must rearrange so as to reduce the activation barrier. The main finding of the current study is that at sufficiently low temperature, ∼160 K, we have detected a sudden decrease in the dynamic part of the solvation energy (occurring on the excited-state potential surface). At $T \geq 200$ K, the dynamic solvation energy is on the order of about 1000 cm^{-1}, whereas at ∼160 K, it is only 200 cm^{-1}. The large decrease in the dynamic solvation energy may explain the previous experimental finding, namely, that the ESPT process is inefficient below 160 K. In excited-state electron-transfer studies,[31,36,37] it was realized that in a glass matrix, the solvation energy is small because of large restrictions and, therefore, the activation barrier and energy are strongly modified, and the yield of the electron-transfer process dramatically decreases below a turnover temperature.

We propose that in the ESPT process, the dynamic part of the solvation energy occurring on the excited-state potential surface is also an important parameter in the determination of the proton-transfer rate. Below 160 K, the excited-state proton transfer is inefficient because the solvation energy drops, and consequently, the rate suddenly decreases.

We have also used coumarin 343 dye (C343) as a probe molecule of the solvation statics and dynamics in methanol-doped ice. This dye had been used in the past in many studies of solvation in aqueous media. The solvation dynamics results of C343 in ice are similar to the one we found with 2N68DS.

Acknowledgment. This work was supported by grants from the Bi-national U.S.−Israel Science Foundation and the James-Franck German−Israel Program in Laser-Matter Interaction.

References and Notes

(1) Horng, M. L.; Gardecki, J.; Papazyan, A.; Maroncelli, M. *J. Phys. Chem.* **1995**, *99*, 17311.
(2) Barbara, P. F.; Jarzeba, W. *Adv. Photochem.* **1990**, *1*, 15.
(3) Simon, J. D. *Acc. Chem. Res.* **1988**, *128*, 21.
(4) (a) Bagchi, B.; Chandra, A. *Adv. Chem. Phys.* **1991**, 1, 80. (b) Bagchi, B. *Annu. Rev. Phys. Chem.* **1989**, *115*, 40.
(5) Ladanyi, B.; Skaf, M. S. *Annu. Rev. Phys. Chem.* **1993**, *335*, 44.
(6) Rosental, S. J.; Xie, X.; Du, M.; Fleming, G. R. *J. Chem. Phys.* **1991**, *95*, 4715.
(7) Bagchi, B. *Annu. Rep. Prog. Chem., Sect. C: Phys. Chem.* **2003**, 99, 127.
(8) Richert R. *J. Chem. Phys.* **2000**, *113*, 8404.
(9) Fletcher, N. H. In *The Chemical Physics and of Ice*; Cambridge University Press: New York, 1970.
(10) Hobbs, P. V. In *Ice Physics*; Clarendon Press: Oxford, U.K., 1974.
(11) Petrenko, V. F.; Whitworth, R. W.; *Physics of Ice*; Oxford University: Oxford, U.K., 1999.
(12) Von Hippel, A.; Runck, A. H.; Westphal, W. B. In *Physics and Chemistry of Ice*; Walley, E., Jones, S. J., Gold, L. W., Eds.; Royal Society of Canada: Ottawa, Canada, 1973; p 236.
(13) (a) Eigen, M. *Angew. Chem., Int. Ed. Engl.* **1964**, *3*, 1. (b) Eigen, M.; Kruse, W.; Maass, G.; De Maeyer, L. *Prog. React. Kinet.* **1964**, *2*, 285.
(14) Kelly, D. J.; Salomon, R. E. *J. Chem. Phys.* **1969**, *50*, 75.
(15) Pauling, L. *J. Am. Chem. Soc.* **1935**, *57*, 2680.
(16) Jaccard, C. *Ann. N.Y. Acad. Sci.* **1965**, *125*, 390.
(17) Bjerrum, N. *Science* **1952**, *115*, 385.
(18) Podeszwa, R.; Buch, V. *Phys. Rev. Lett.* **1999**, *83*, 4570.
(19) Leiderman, P.; Uritski, A.; Huppert, D. *J. Phys. Chem. A* **2007**, *111*, 4998.
(20) Kamlet, M. J.; Abboud, J. L. M.; Abraham, M. H.; Taft, R. W. *J. Org. Chem.* **1983**, *48*, 2877.
(21) Laurence, Ch.; Nicolet, P.; Datali, M. T.; Abboud, J. L. M.; Notario R. *J. Phys. Chem.* **1994**, *98*, 5807.
(22) Solntsev, K. M.; Huppert, D.; Tolbert, L. M.; Agmon, N. *J. Am. Chem. Soc.* **1998**, *120*, 7981.
(23) Solntsev, K. M.; Huppert, D.; Agmon, N. *J. Phys. Chem. A* **1998**, *102*, 9599.
(24) Correa, M. N.; Levinger, N. *J. Phys. Chem. B* **2006**, *110*, 13050.
(25) Stavrov, S.; Huppert, D.; Solntsev, K. M.; Dong, J.; Tolbert, L. M. *J. Am. Chem. Soc.* **2006**, *128*, 1540.
(26) Kosower, E. M.; Huppert, D. *Chem. Phys. Lett.* **1983**, *96*, 433.
(27) Kosower, E.; Huppert, D. *Annu. Rev. Phys. Chem.* **1986**, *37*, 122.
(28) Maroncelli, M. *J. Mol. Liq.* **1993**, *57*, 1.
(29) Cohen, B.; Leiderman, P.; Huppert, D. *J. Phys. Chem. A* **2002**, *106*, 11115.
(30) Kobayashi, C.; Saito, S.; Ohmine, I. *J. Chem. Phys.* **2001**, *115*, 4742.
(31) Matyushov, D. V., *Acc. Chem. Res.* **2007**, *40*, 294..
(32) Petrenko, V. F.; Whitworth, R. W. *The Physics of Ice*; Oxford University: Oxford, U.K., 1999; Chapter 11.8.
(33) Richert, R.; Stickel, F.; Fee, R. S.; Maroncelli, M. *Chem. Phys. Lett.* **1994**, *229*, 302.
(34) Johari, G. P.; Whalley, E. *J. Chem. Phys.* **1981**, *75*, 1333.
(35) Kawada, S.; Tutiya, R. *J. Phys. Chem. Solids* **1997**, *58*, 115.
(36) Goes, M.; de Groot, M.; Koeberg, M.; Verhoeven, J. W.; Lokan, N. R.; Shephard, M. J.; Paddon-Row, M. N. *J. Phys. Chem. A* **2002**, *106*, 2129.
(37) Sumi, H.; Marcus, R. A. *Acc. Chem. Res.* **1990**, *23*, 294.